Fault localization on power cables using time delay estimation of partial discharge signals

Chin Kui Fern[1,2], Chai Chang Yii[1], Asfarina Abu Bakar[1, 2], Ismail Saad[1], Kenneth Teo Tze Kin[1], Megat Muhammad Ikhsan Megat Hasnan[1], Nur Aqilah Mohamad[1]
[1]Faculty of Engineering, Universiti Malaysia Sabah, Kota Kinabalu, Malaysia
[2]Faculty of Engineering and Technology, i-CATS University College, Kuching, Malaysia

Article Info

ABSTRACT

Precise localization of partial discharge (PD) sources on power cables is vital to prevent power line failures that can lead to significant economic losses for electrical suppliers. This study proposes four methods to estimate the time delay of PD signals under electromagnetic interference, including white Gaussian noise (WGN) and discrete sinusoidal interference (DSI), using denoised PD signals with signal-to-noise ratios ranging from 10.6 to -7.02 dB. The maximum peak detection (MPD) and cross-correlation (CC) approaches, as well as two new techniques, interpolation cross-correlation (ICC) and envelope cross-correlation (ECC), are evaluated for their effectiveness in PD source localization. The researchers employ the time difference of arrival (TDoA) algorithm to compute PD location using the double-end PD location algorithm, where the PD location precision serves as an indicator of the accuracy of the time delay estimation methods. The study concludes that CC and ICC are the most suitable methods for estimating the time delay of PD signals in the PD location algorithm, as they exhibit the lowest error rates. These results suggest that CC and ICC can be used effectively for precise PD source localization under electromagnetic interference on power cables.

Corresponding Author:

Chai Chang Yii
Faculty of Engineering, Universiti Malaysia Sabah
UMS Street, 88400 Kota Kinabalu, Sabah, Malaysia
Email: chaichangyii@ums.edu.my

1. INTRODUCTION

The reliability of power systems is of utmost importance, and the timely detection of faults in electrical equipment and cables is crucial for maintaining this reliability. According to IEC-60270, partial discharge (PD) refers to a local dielectric breakdown that occurs in a small part of an insulation system when the local electric field exceeds the local dielectric strength at a specific location in or near an energized object [1]. The occurrence of PD can be attributed to factors such as contamination, aging, or damage to the insulating material between different voltage potentials, which can lead to gradual damage and eventual failures. Hence, reliable and non-intrusive PD localization methods are necessary for detecting and locating PD signals. These methods can be performed online during routine servicing or offline by energizing each successive phase with a high-voltage source [2]. Table 1 illustrates some of the available methods for PD detection [3].

The process of PD location comprises three sub-processes that are critical to its success, as illustrated in Figure 1. The first sub-process is the detection of the PD at the sensor, which is extensively discussed [4]. The second sub-process involves the application of de-noising techniques to eliminate electromagnetic noise, as described in [5]. Finally, the time difference of arrival (TDoA) method is used to locate the PD [6].

Table 1. PD detection methods with their advantages, disadvantages, and applications

PD detection methods	Description	Advantages	Disadvantages	Application
Ultra-high frequency (UHF) measurement [7], [8]	- Measuring the UHF electromagnetic signals emitted by PD events in the UHF frequency range (300 MHz to 3 GHz). - Example of sensors used: Antennas, coaxial cables, and resonant circuits.	- High sensitivity - Capability to detect PD events in real time. - Ability to detect PDs in the early stage of insulation deterioration. - Can be performed remotely.	- Measurement ranges are restricted - The requirement for specialized equipment. - The potential for interference from other sources - The potential for measurement errors due to reflections and multi-path effects.	- High-voltage electrical equipment, such as power transformers, gas-insulated switchgear, and cables.
Acoustic measurement [9]–[11]	- Measuring the sound waves generated by the discharge, which can be detected by sensors placed in close proximity to the insulation. - Example of sensors used: Ultrasonic sensors, airborne and structure-borne sensors.	- Low cost - Capability to detect PD events in real-time - Can detect PD in a wide range of insulation types, including solid, liquid, and gas-insulated systems. - Can provide information on the location and severity of the discharge. - Can detect PD in both high and low-voltage equipment.	- Low sensitivity - Difficulty in accurately locating the source of PD - Can be affected by external noise such as background noise in the environment. - The signal strength can be affected by the distance between the sensor and the insulation. - May be necessary to use multiple sensors to cover a large area.	- High-voltage electrical equipment, such as power transformers, gas-insulated switchgear, and cables. - Use in aerospace and automotive, for detecting PD in insulation systems used in motors, generators, and other electrical equipment.
Optical detection [12], [13]	- Detects ultraviolet (UV) and visible light generated by discharge events with optical sensors. - Examples of sensors used: Photomultiplier tubes (PMTs) or photodiodes.	- High sensitivity, - Can detect even low-level PD events and provide accurate measurements of the discharge magnitude, location, and frequency. - Does not require any direct contact with the insulation, which is beneficial for online monitoring applications.	- Expensive, - Complex to operate, - The impact of ambient light, and the potential for sensor saturation due to high light levels. - UV light can be harmful to humans, so proper safety precautions must be taken when working with optical PD sensors.	- Online monitoring of high-voltage equipment such as transformers, cables, and switchgear
Impedance measurement [14]	- Measuring the electrical system's impedance to detect the presence of PD events. - Example of sensors: Capacitive sensors	- Can detect PD in a wide range of insulation types, including solid, liquid, and gas-insulated systems. - Real-time detection of PD events - Capability to identify and locate PD events in complex electrical systems. - Less affected by external noise sources, more reliable in noisy environments.	- The requirement for specialized equipment. - May not be able to detect very low-level PD signals. - May not provide information on the location or severity of the discharge.	- High-voltage electrical equipment, such as power transformers and cables.
Thermal imaging [15]	- Detecting heat generated by PD events with infrared cameras, which can be seen as hot spots on the surface of the equipment. - Example of sensors: - Infrared sensors or cameras.	- High sensitivity - Capability to visualize PD events - Invasive nature, it does not require the equipment to be taken out of service for testing. - Can detect PD activity in inaccessible or hard-to-reach areas.	- The requirement for specialized equipment. - The possibility of false readings in the presence of thermal noise. - Can only detect surface PD activity, it may not be able to detect PD activity within the insulation system.	- High-voltage electrical equipment, such as power transformers and switchgear used in the aerospace industry.

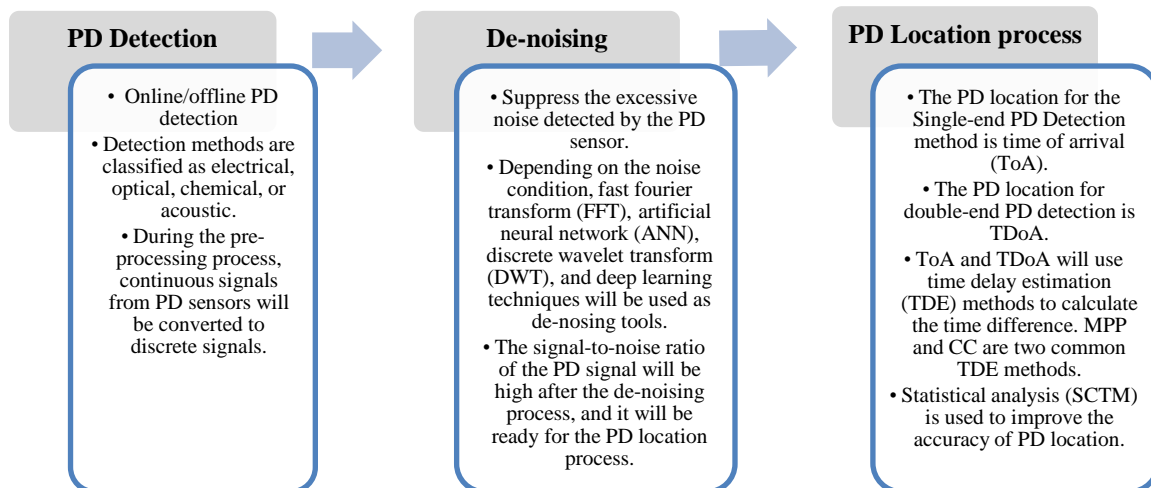| PD Detection		De-noising		PD Location process
• Online/offline PD detection • Detection methods are classified as electrical, optical, chemical, or acoustic. • During the pre-processing process, continuous signals from PD sensors will be converted to discrete signals.	→	• Suppress the excessive noise detected by the PD sensor. • Depending on the noise condition, fast fourier transform (FFT), artificial neural network (ANN), discrete wavelet transform (DWT), and deep learning techniques will be used as de-nosing tools. • The signal-to-noise ratio of the PD signal will be high after the de-noising process, and it will be ready for the PD location process.	→	• The PD location for the Single-end PD Detection method is time of arrival (ToA). • The PD location for double-end PD detection is TDoA. • ToA and TDoA will use time delay estimation (TDE) methods to calculate the time difference. MPP and CC are two common TDE methods. • Statistical analysis (SCTM) is used to improve the accuracy of PD location.

Figure 1. PD location processes

Partial discharge diagnosis is a crucial component of electrical insulation testing. Several sensor techniques [16] have been developed to accomplish this goal, including the UHF method [17], optical acoustic technology [18], acoustic analysis [19], high-frequency current transformers (HFCTs) [20]–[22], Rogowski Coils [23], [24], and capacitive sensors [25]. Each of these methods has its own strengths and weaknesses. The selection of a sensor depends on several factors such as the type of partial discharge being analyzed, the ambient conditions, and the desired measurement accuracy and sensitivity.

Detecting and extracting PD signals amidst noisy environments during on-site PD measurements poses a significant challenge. The presence of noise sources, such as thermal or resistive noise from measuring circuits and high-frequency sinusoidal signals that are electromagnetically coupled, make the task even more difficult. Precise and reliable detection of PD signals requires the implementation of advanced deep learning techniques [26], [27]. To accurately detect PD signals, the TDoA of an UHF signal emitted by a partial discharge source can be calculated and detected. The first peak and cumulative energy methods, presented in [28], provide effective means for calculating and detecting TDoA. With the use of these techniques, the TDoA of the UHF signal can be precisely determined, thereby enabling the accurate detection of PD signals.

PD localization algorithms can improve power system reliability by detecting insulation problems in cables and power equipment in a substation. Numerous PD localization algorithms have been developed in recent years, including "UHF partial discharge localization algorithm" [29], [30], "partial discharge localization in high voltage systems" [31] "partial discharge localization method in transformers" [32], multi-end correlation-based PD location technique (MEC) [33], segmented correlation and trimmed mean data filtering techniques for medium-voltage (MV) underground cable segmented correlation trimmed mean (SCTM) [34] and others. According to recent research, SCTM [34] outperforms the MEC algorithm in terms of PD location accuracy. The careful selection of a PD localization algorithm is crucial for improving the accuracy of the diagnosis of insulation problems in cables and power equipment, and thus enhancing the reliability of the power system.

This research aims to improve the accuracy and reliability of PD localization algorithms for power cables by investigating the best time delay estimation method. Some of their characteristics are lost during the denoising process when PD signals are in a high-noise environment. The aim of this study is to compare the performance of four-time delay estimation methods [35], [36], apart from the commonly used approaches maximum peak detection (MPD) and cross-correlation (CC), two new methods are also introduced by the authors, namely interpolation cross-correlation (ICC) and envelope cross-correlation (ECC) to determine the most effective approach. The results of this research have the potential to enhance the reliability of power systems.

2. METHOD

The proposed research study entails the utilization of MATLAB scripting to perform simulations aimed at evaluating the effects of four distinct time delay estimation methods on the online PD monitoring system under scrutiny. Figure 2 shows the proposed online PD monitoring system that utilizes a double-end PD sensor measuring method to estimate the PD location. This system may employ Rogowski coil (RC) or

HFCT as high-precision and non-intrusive sensors to capture the PD signal. However, due to the limitations of HFCT in saturation, size, weight, and cost [37], coreless inductive sensors in the form of Rogowski coils are preferred due to their ease of construction and maintenance, light design, compact size, low cost, and fast response [38]. The RC sensor captures a 100 microseconds length signal window and has a 10 MHz sampling frequency that generates 10,000 data samples per window. Measured signals from PD Sensor A and PD Sensor B are transmitted to the substation's receiver for PD monitoring and estimation. The substation's data acquisition unit estimates the PD location on the power cable using the double-end PD location algorithm, which involves signal de-noising, time delay estimation, and PD location estimation.

The PD location algorithm's process flow is illustrated in Figure 3. Initially, the PD monitoring system imports the measured signal windows from PD sensor A (Window A) and PD sensor B (Window B). To ensure the accuracy and reliability of the PD location estimation process, the proposed methodology involves a comprehensive approach shown in Figure 3 verifies the presence of the PD signal, selects the most effective method for estimating the time delay, and uses the TDoA to estimate the PD location. These steps are critical for ensuring the accuracy and reliability of the PD location estimation process.
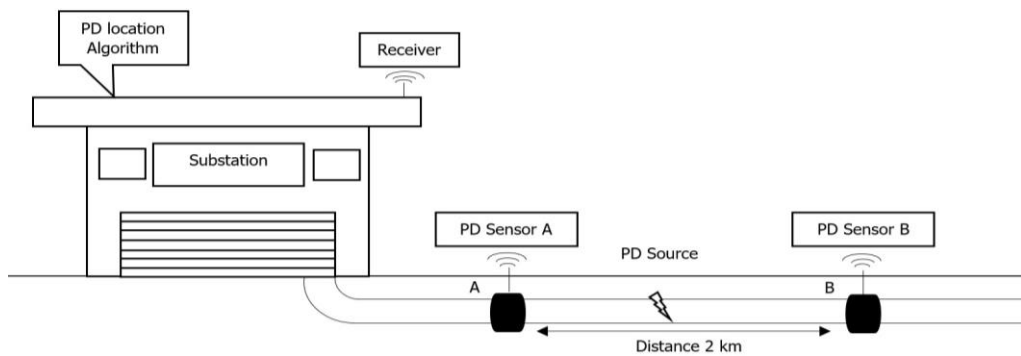

Figure 2. Diagram of the online PD localization estimation system using double-end PD sensor measuring method [39]
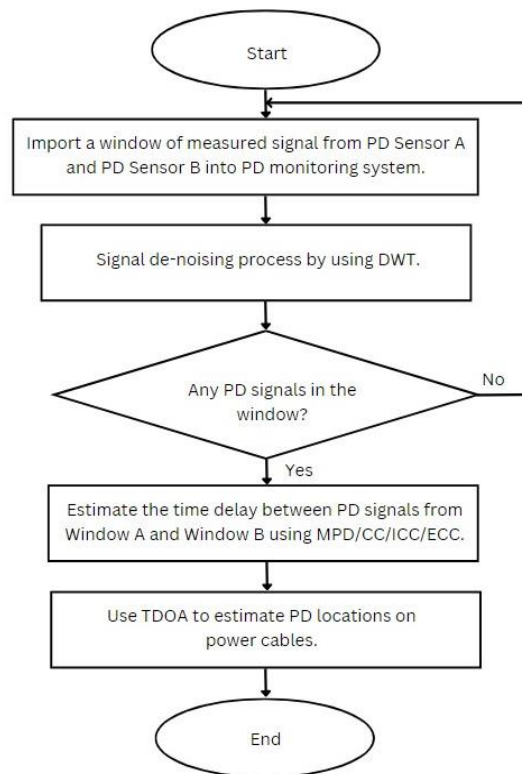

Figure 3. Process flow of PD location algorithm

The de-noising process is carried out using the DWT Daubechies 3 (db 3) mother wavelet and decomposition filter value of 4 to eliminate the effect of DWT de-noising on time delay estimation accuracy. The decision to utilize db 3 as a mother wavelet for DWT de-noising is supported by its favorable attributes, which include a well-balanced combination of time and frequency localization, as well as a relatively smooth and compact support. Additionally, the use of a decomposition filter value of 4 in DWT de-noising enables efficient multi-resolution analysis of the signal, resulting in enhanced noise reduction while still preserving important signal characteristics. The de-noising process is illustrated in Figure 4, which shows Figure 4(a) a signal with -0.764 dB SNR, Figure 4(b) a denoised signal using DWT, and Figure 4(c) an absolute denoised signal. The absolute signal is utilized because the negative side of the signal may lead to an inaccurate cross-correlation coefficient profile.
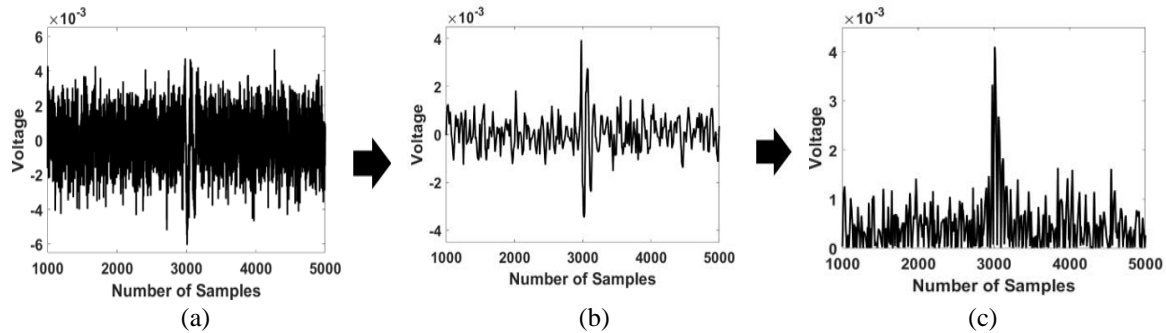

Figure 4. DWT de-nosing and absolute process, (a) pre-processing measured PD signals that have been corrupted by white gaussian noise (WGN) and discrete sinusoidal interference (DSI), (b) post-processing denoised PD signal after DWT noise suppression, and (c) post-processing absolutely denoised PD signal after absolute processing

The PD location algorithm will verify the presence of the PD signal in the denoised signal. If a PD signal is present, the time delay estimation process continues; otherwise, a new Window A and Window B are imported. Second, the estimated time delay between high-similarity PD signals from Window A and Window B is determined using four different methods, namely MPD, CC, ICC, and ECC. The effectiveness of these methods is evaluated to determine the most effective technique for estimating the PD location between two PD signals. Finally, TDoA is employed to estimate the PD location based on the estimated time delay. The estimated PD location, L_{pd} is obtained by applying (1).

$$L_{pd} = L - 1/2(L - v * t_d) \tag{1}$$

where L is the total cable length, v is the velocity of PD signal propagating along the cable, and t_d is the estimated time difference between two PD signals from Window A and Window B.

The velocity of a PD signal as it travels through an underground cable is influenced by the cable's semiconducting and dielectric screen layers. As shown in (2) [39], [40] defines the propagation velocity of the PD signal along the cable v as (2).

$$v_f = {v_s}/{\sqrt{\varepsilon}} \tag{2}$$

where v_s is propagation velocity in free space (300 m/μs), and ε is effective relative permittivity of the cable's dielectric and semiconducting screen layers.

2.1. Noise modeling

In practical scenarios, PD sensors can be susceptible to two types of interference: WGN and DSI. WGN is a stochastic signal characterized by a Gaussian probability distribution and flat power spectral density across all frequencies, it is identified by its amplitude which conforms to a normal or Gaussian probability density function [41]. WGN is commonly used as a reference signal in signal processing and communication systems and can be generated synthetically through the use of a random number generator. Notably, WGN can be generated using the 'awgn' function in MATLAB. DSI is periodic interference with a specific frequency

introduced into a signal by external sources, such as electrical or electromagnetic interference. It is characterized by a sinusoidal waveform and can cause distortions or disruptions in the signal, affecting the accuracy and reliability of signal processing or communication systems. DSI signals, on the other hand, can be generated using the sinusoidal equation presented in (3) [33]. In this case, four different frequencies of DSI signals are generated, which are $f_1 = 600$ kHz, $f_2 = 800$ kHz, $f_3 = 1.5$ MHz, and $f_4 = 5$ MHz.

$$DSI(t) = A_{max} \sum_{t=1}^{N} 2\pi f_i t \tag{3}$$

where A_{max} is amplitude of the DSI range from 0.05 to 0.5 mV in intervals of 0.05 mV, and f_i is frequencies used to generate the DSI signal.

2.2. MPD method

In estimating the time delay using the MPD method, the denoised signal obtained from Window A and Window B is subjected to an absolute operation to convert the negative portion of the signal to the positive side. Subsequently, the MATLAB function "max" is then utilized to determine the maximum point in the time series measured signal for both Window A and Window B, denoted as $A_{max,A}$ and $A_{max,B}$, respectively. The time delay between two identical PD signals, t_d can be determined using (4). Based on the estimated time delay, the approximate location of the PD on the power cable can be calculated using (1).

$$t_d = t_{max,A} - t_{max,B} \tag{4}$$

where $t_{max,A}$ is the time at which the measured signal A reaches its maximum point, $A_{max,A}$ and $t_{max,B}$ is the time at which the measured signal B reaches its maximum point, $A_{max,B}$.

2.3. CC method

The CC method is a widely used signal processing method for determining the similarity of two sets of time-domain PD signals, and is often employed in estimating time delay. The general CC function for a continuous signal is defined as (5) [42].

$$R_{AB}(\tau) = \lim_{T \to \infty} \frac{1}{T} \int_0^T A(t + \tau)B(t)dt \tag{5}$$

where $A(t)$ and $B(t)$ are two samples of the signal.

However, the signal output from measuring devices is often discrete, and the corresponding discrete CC equation is defined as (6).

$$R_{AB} = \sum_0^n A[n] \times B[n] \tag{6}$$

where $A[n]$ and $B[n]$ are two signals from Window A and Window B, n is the number of samples in a window, and R_{AB} is the CC coefficient.

To estimate the time delay of discrete PD signals from Window A and Window B using the CC method, the absolute denoised signals from Window A are multiplied, added, and circularly shifted with the denoised signals from Window B until the Window A sample is circularly shifted in a full cycle. Window B will remain unshifted because it is selected as the reference for Window A. This process generates a CC coefficient profile. The number of CC coefficient profile samples is the same as the number of Window A or Window B samples. If the number of samples that produce the maximum point from the CC coefficient profile, n_{max} is less than half of the CC coefficient profile samples, n, then (7) is used to compute the sample delay between PD signals at Window A and PD signals at Window B, n_d. Otherwise, (8) will be used to compute n_d. The time delay between the PD signals in Window A and those at Window B, denoted as t_d, can be calculated using (9). The estimated location of PD on the power cable can be computed using (1).

$$n_d = -n_{max} \tag{7}$$

$$n_d = n - n_{max} \tag{8}$$

$$t_d = n_d \times T \tag{9}$$

where T is the time interval between two samples and $T = 1/_{Sampling\ frequency}$.

2.4. ICC method

The ICC method is a novel approach proposed by the authors to enhance the accuracy of time delay estimation, and consequently improve the accuracy of PD location estimation. The primary concept of the ICC method is to increase the area of the PD signal for the CC process. This method comprises three distinct stages, namely peak finding, linear interpolation, and the CC process.

In the first stage, as depicted in Figure 5(a), the absolute denoised signals from Windows A and B undergo a peak finding process. To identify the peaks in the absolute denoised signals, the 'findpeaks' function of MATLAB is utilized, as shown in Figure 5(b). After the peak finding process, Window A and B will retain the peak samples, while the remaining samples will be discarded. Thus, a linear interpolation process is required to linearly interpolate the eliminated samples based on the peak samples.

Figure 5(c) displays the results of the linear interpolation process. During the second stage, the linear interpolation process is carried out using the 'fillmissing' function in MATLAB. The 'fillmissing' function uses linear interpolation to fill in the gaps between the peaks. A linear equation is required between two adjacent peak samples A and B, as shown in Figure 6. The linear interpolation equation can be defined as (10),

$$y = mx + c \tag{10}$$

where y is the voltage of the PD signal in the y-axis, x is the sample number in the x-axis, m is the slope of the linear line, and c is the value of y when the linear line intersects at the origin.

The linear equation can be easily determined by substituting the coordinate of two adjacent peaks $A(x_1, y_1)$ and $B(x_n, y_n)$. After the linear equation is determined, the gaps between peaks can be filled by substituting the sample's value, x into (10). The interpolation process is repeated for all of the gaps between peaks.

In the third stage, the CC process is applied to the interpolated signals from Windows A and B, as described in subsection 2.2. This stage utilizes the CC function defined in (6) to estimate the time delay between the PD signals from Window A and Window B. The estimated location of PD on the power cable can be computed using (1).
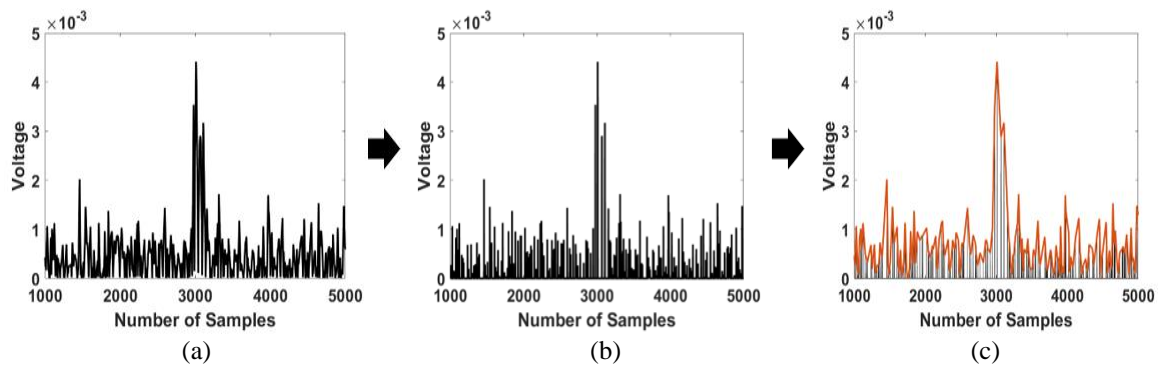

Figure 5. Linear interpolation of peaks process: (a) absolute denoised PD signal as input to linear interpolation process, (b) absolute denoised PD signals local peak identification in (c) post-processing linear interpolation of absolute denoised pd signal local peak
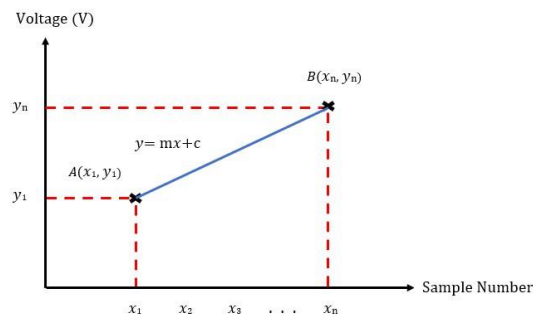

Figure 6. Linear interpolation of peak samples

2.5. ECC method

The authors also proposed another new approach, the ECC method, comprising two distinct processes: the envelope and the CC process. Initially, the absolute denoised signals obtained from Window A and Window B are subjected to the envelope process using the 'envelope' function available in MATLAB. The envelope of a signal is a smooth curve outlining the upper and lower bounds of the signal's amplitude, as illustrated in Figure 7. The envelope process allows for the identification of the peaks in the signals, which are then utilized in the subsequent CC process. Figure 7(a) displays the absolute denoised PD signal utilized as input for the envelope process. Figure 7(b), on the other hand, presents the result of the post-processing absolute denoised PD signal after the envelope process.

As described in subsection 2.2, the CC process involves calculating the CC coefficient profile by multiplying, adding, and circularly shifting the signals from Windows A and B. In the ECC method, the CC process is applied to the enveloped signals rather than the raw signals. This allows for the identification of the peaks in the signals, which are then utilized in the CC process to increase the accuracy of time delay estimation and PD location estimation.

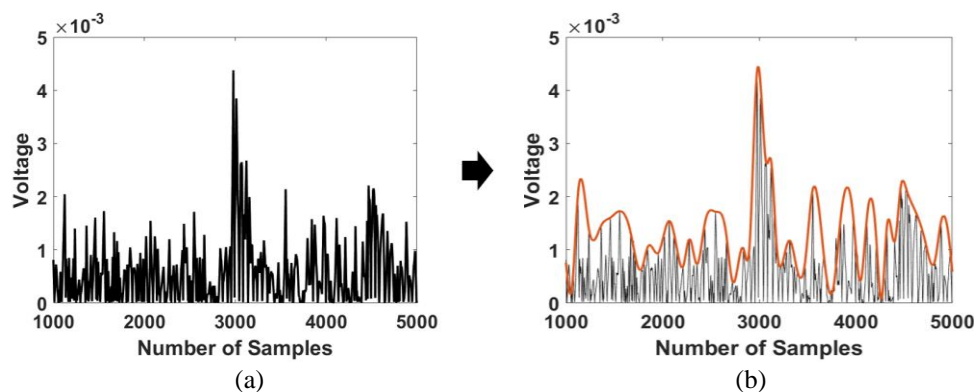(a)   (b)

Figure 7. Envelope process (a) absolute denoised PD signal as input to envelope process and (b) post-processing of absolute denoised PD signal after envelope process

3. RESULTS AND DISCUSSION

In this section, the simulation results for DWT de-noising and percentage error of the PD location algorithm using MPD, CC, ICC, or ECC as time delay estimation methods for PD signals at Window A and Window B are presented. The most accurate method for PD location estimation is identified by analyzing and discussing the results. In subsection 3.1, the impact of DWT de-noising using Daubechies 3 mother wavelet and decomposition filter value of 4 is compared. Subsection 3.2 compares the average percentage error of the PD location algorithm using different time delay estimation methods. Similarly, subsection 3.3 compares the maximum percentage error of the PD location algorithm across the different methods.

3.1. DWT De-noising

To evaluate the effectiveness of DWT de-nosing technique in suppressing noise, WGN and DSI were added into Window A and Window B with signal-to-noise ratios (SNRs) ranging from 10.6 to -7.02 dB. Figure 8 depicts signals with varying levels of noise, and it is observed that the PD signal is still visible when the noise level is low, as demonstrated in Figure 8(a) and 8(b). However, when the noise level is high, as shown in Figure 8(c) to 8(f), the efficacy of the DWT denoising technique becomes significant in suppressing the noise. As depicted in Figure 9(a) to 9(d), DWT can effectively suppress noise, whereas in Figure 9(e) to 9(f), it is noticeable that DWT's noise suppression performance decreases. Therefore, a reliable time delay estimation method is essential in determining the time delay between two PD signals in Window A and Window B even if the noise in the PD signal cannot be entirely suppressed.

3.2. Comparison of average percentage error

The simulation results presented are based on a pre-determined PD location occurring 1.5 km away from the front end of the monitored cable. The simulation was conducted on a specific medium-voltage three-core monitored cable (50 mm^2 Cu/XLPE/PVC, 8.7/15 kV) with PD sensors sampling at a frequency of 100 MHz, a PD signal propagation velocity, v of 156.07 m/us as established in [40]. The PD locations algorithm that employs MPD, CC, ICC, and ECC as time delay estimation methods, was executed 100 times

for SNRs ranging from 10.6 dB to -7.02 dB to generate average PD location samples. The mean of these 100 samples is shown in Table 2, which indicates the SNR and average PD location obtained using MPD, CC, ICC, and ECC algorithms for 10 different noise amplitudes. The amplitude of DSI noise was incrementally raised from 0.05 to 0.50 mV in 0.05 mV intervals, while the amplitude of WGN was decreased in intervals of -2 dB, ranging from 0 to -18 dB. The SNR was then computed by adding the noise to the PD signals using (11) and (12) [43]:

$$SNR = (\frac{A_{signal}}{A_{noise}})^2 \tag{11}$$

where A_{signal} is the amplitude of the PD signal, and A_{noise} is the amplitude of the noise.

$$SNR_{dB} = 10log_{10}(SNR) \tag{12}$$
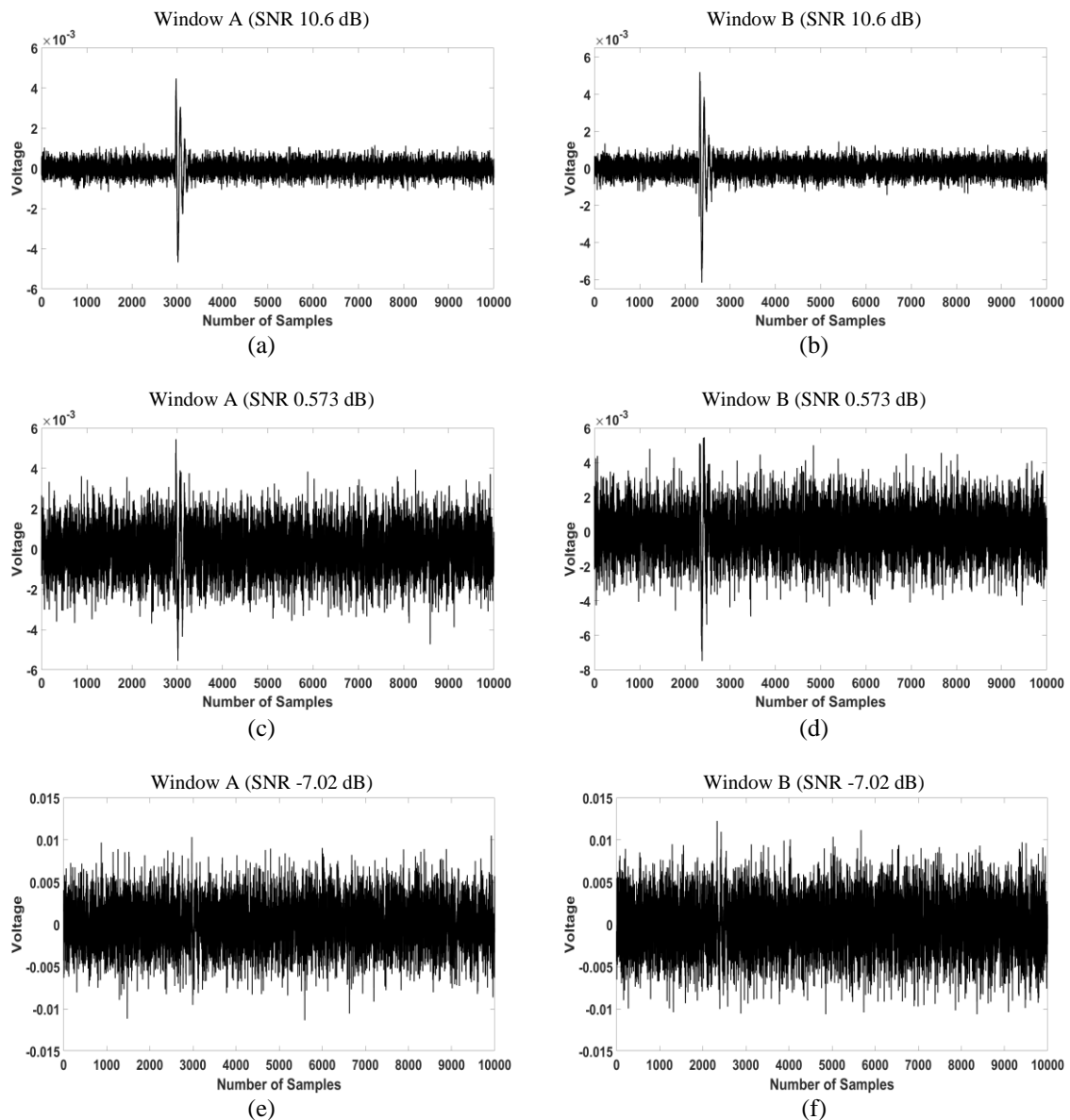
Figure 8. Varies level of WGN and DSI noises: (a) measured PD signal with 10.6 dB noises from Window A, (b) measured PD signal with 10.6 dB noises from Window B, (c) measured PD signal with 0.573 dB noises from Window A, (d) measured PD signal with 0.573 dB noises from Window B, (e) measured PD signal with -7.02 dB noises from Window A, and (f) measured PD signal with -7.02 dB noises from Window B
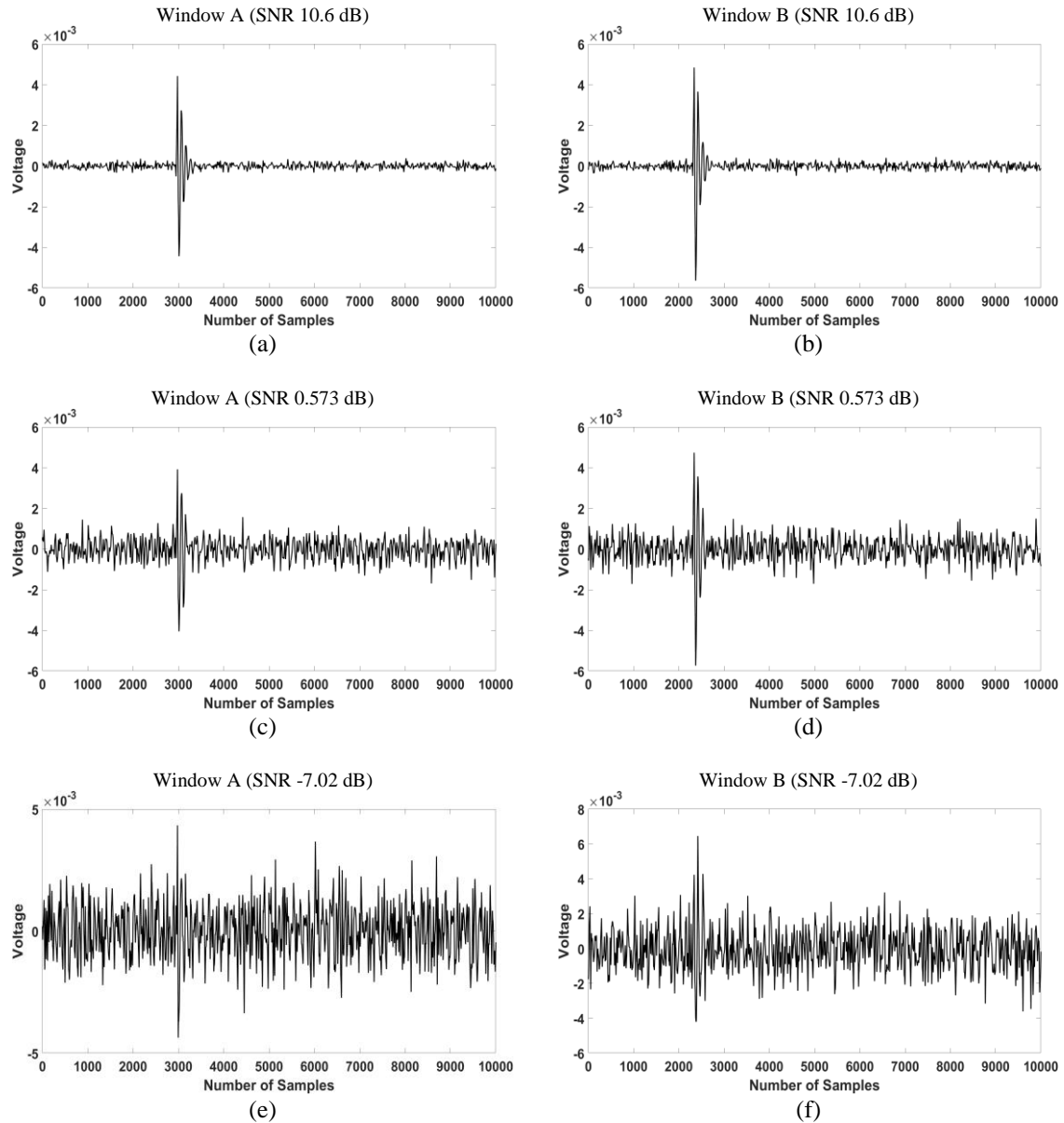
Figure 9. Denoised signal by using DWT de-noising technique: (a) denoised DWT PD signal with 10.6 dB noises from Window A, (b) denoised DWT PD signal with 10.6 dB noise from Window B, (c) denoised DWT PD signal with 0.573 dB noise from Window A, (d) denoised DWT PD signal with 0.573 dB noise from Window B, (e) denoised DWT PD signal with -7.02 dB noise from Window A, (f) denoised DWT PD signal with -7.02 dB noise from Window B

Table 2. The average percentage error of PD location using MPD, CC, ICC, and ECC as time delay estimation methods, respectively

Noise (mV)	SNR	SNR (dB)	CC	ECC	MPD	ICC
1.4586	11.5000	10.6000	0.0115	0.2869	0.1189	0.0119
1.9315	6.5400	8.1600	0.0124	0.3744	0.1055	0.0128
2.0505	5.8000	7.6400	0.0137	0.4096	0.2456	0.0136
3.2322	2.3400	3.6800	0.0151	0.5008	0.2581	0.0158
3.6550	1.8300	2.6200	0.0206	0.5765	0.4375	0.0166
4.6244	1.1400	0.5730	0.0214	0.7453	0.5360	0.0196
5.3942	0.8390	-0.7640	0.0209	0.8498	1.6210	0.0209
6.7383	0.5370	-2.7000	0.7147	13.6056	5.0293	4.3979
8.5534	0.3340	-4.7700	15.1865	34.0694	14.3452	32.6360
11.0878	0.1980	-7.0200	54.8256	59.4435	41.9539	64.7926

The results in Table 2 demonstrate that the average percentage error of PD location using MPD, CC, ICC, and ECC increases as the SNR in the dB unit decreased. This is due to the increased noise in Window A and Window B obscuring the PD signals, thereby reducing the accuracy of time delay estimation and increasing the percentage error of PD location. As a result, the accuracy of time delay estimation will be reduced, while the percentage error of PD location will increase. A reliable time delay estimation method can, therefore, reduce the percentage of PD location error.

To demonstrate the effectiveness of four different time delay estimation methods in reducing the percentage error of PD location, a comparison graph was drawn based on Table 2, shown in Figure 10. The results in Figure 10 demonstrate that the ECC method has the highest error percentage due to the enveloping process used in ECC, reducing the similarity between the PD signals from Window A and Window B and leading to inaccurate time delay computation. The MPD method has the second-highest error percentage, as it can accurately calculate the time delay between PD signals when the SNR is high and the PD signals retain their perfect shape. However, when the SNR decreases to 0.573 dB or lower, the PD shape is attenuated, making the MPD method unreliable. In contrast, the CC and ICC methods perform well in the time delay estimation process, as evidenced by the average percentage error of PD location remaining under 0.02% even as the SNR value decreases up to -0.764 dB. Specifically, the CC and ICC methods show an average percentage error reduction of at least 98.65% and 97.54%, respectively, compared to the MPD and ECC methods for the SNR equal to -0.764 dB.

Figure 11 presents a zoomed-in comparison graph of the CC and ICC methods. As shown in Figure 10, the CC and ICC methods perform similarly well when the SNR is higher than 0 dB. However, when the SNR decreases to -2 dB and below, the average PD location percentage error using the ICC method increases slightly more than when using the CC method. Nevertheless, both methods are able to maintain the average PD location percentage error below 0.02% when the SNR is -0.764 dB. In conclusion, the results indicate that the CC and ICC methods perform well in the time delay estimation process, and can reduce the percentage of PD location error. These findings may have practical implications for PD location systems in the field of power systems engineering.
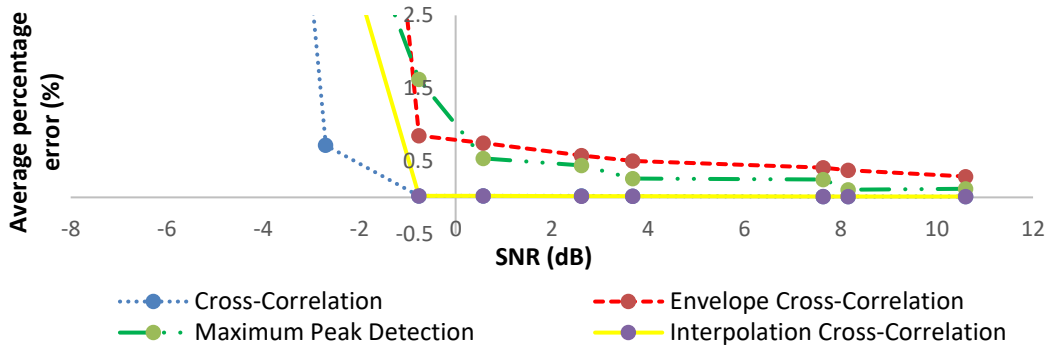

Figure 10. Comparison of the average percentage error in PD location estimation methods MPD, CC, ICC, and ECC
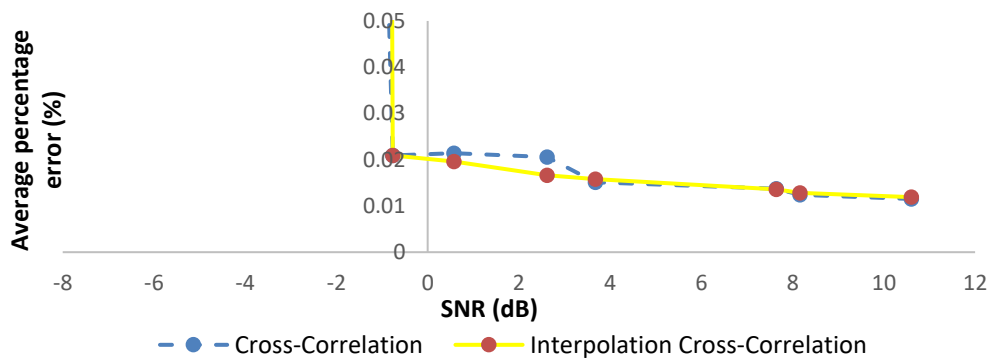

Figure 11. Comparison of PD location average percentage error by applying CC and ICC time estimation methods

3.3. Comparison of maximum percentage error

The maximum percentage error of PD location is another important criterion to consider when evaluating the effectiveness of time delay estimation methods in the PD location algorithm. In this section, the effectiveness of the PD location algorithm was evaluated using four different time delay estimation methods, namely MPD, CC, ICC, and ECC, under various SNR conditions ranging from 10.6 to -7.02 dB. The algorithm was run 100 times to find the maximum percentage error of PD location among the 100 estimated samples. Table 3 summarizes the results obtained from this analysis, indicating that the maximum percentage error of PD location follows a similar trend to the average percentage error, where both errors increase as the SNR decreases in the dB unit.

A comparison graph was drawn based on the results presented in Table 3, and Figure 12 illustrates the effectiveness of the different time delay estimation methods under varying SNR conditions. The ECC method was found to be inaccurate for SNR values less than -0.764 dB, while the MPD method was inaccurate for SNR values less than -0.573 dB. The zoomed-in graph shown in Figure 13 further reveals that the CC and ICC methods have the same maximum percentage error (0.05%) until the SNR reaches 2.62 dB. To further reduce the percentage error, a trimmed mean data filtering technique, as described in [35], can be used. However, conducting field experiments is necessary to validate the effectiveness of the CC and ICC methods in time delay estimation.

Table 3. The maximum percentage error of PD location using MPD, CC, ICC, and ECC as time delay estimation methods, respectively

| Noise (mV)	SNR	SNR (dB)	CC	ECC	MPD	ICC
1.4586	11.5000	10.6000	0.0288	1.3164	1.3164	0.0288
1.9315	6.5400	8.1600	0.0288	1.3944	1.3164	0.0288
2.0505	5.8000	7.6400	0.0288	1.4725	1.3164	0.0288
3.2322	2.3400	3.6800	0.0492	1.7846	1.3164	0.0492
3.6550	1.8300	2.6200	0.0492	1.7456	1.3368	0.0492
4.6244	1.1400	0.5730	0.0883	2.2528	1.8440	0.0678
5.3942	0.8390	-0.7640	0.0678	2.6820	59.9021	0.0678
6.7383	0.5370	-2.7000	58.6145	161.0540	121.0425	142.3256
8.5534	0.3340	-4.7700	214.7811	197.8865	200.3651	181.0700
11.0878	0.1980	-7.0200	219.8534	218.7999	255.3017	197.9646
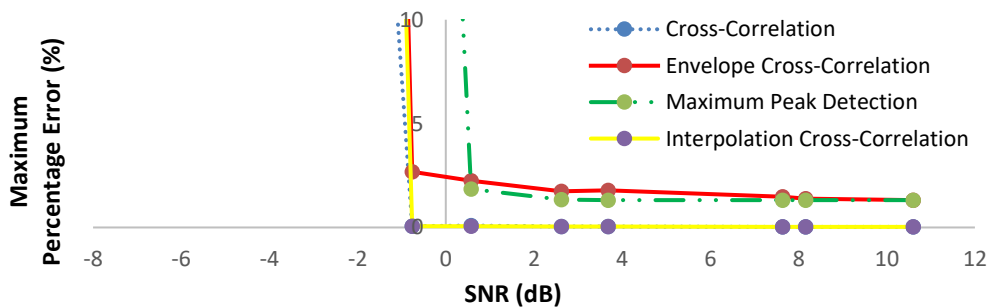
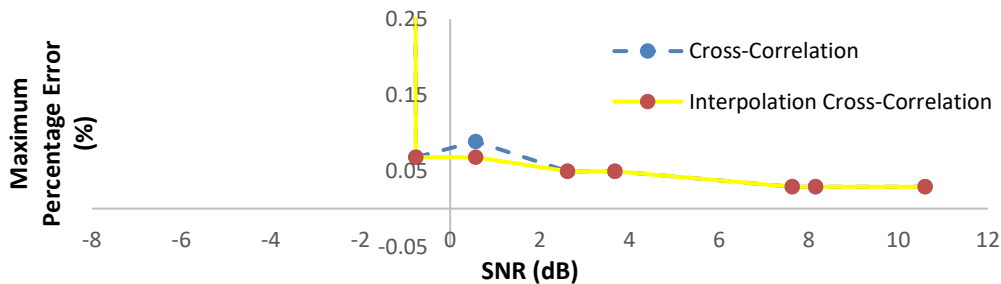Figure 12. Comparison of PD location maximum percentage error estimation methods using MPD, CC, ICC, and ECC

Figure 13. Comparison of PD location average percentage error by applying CC and ICC time estimation methods

4. CONCLUSION

In summary, our research compared four different time delay estimation methods (the MPD, CC, ICC, and ECC methods). The simulations were used to quantify the performance of the proposed methods. The statistical results demonstrate that increasing noise level reduced the accuracy of time delay estimation, resulting in higher PD location estimation errors. Furthermore, when PD signals were heavily polluted with WGN and DSI, both the CC and ICC methods were more efficient than the MPD and ECC methods, with more than 90% average percentage error reduction. Our research provides valuable insights into the performance of different time delay estimation methods under varying levels of noise. These findings have important implications for applications such as PD location detectors and could inform the development of more accurate and efficient methods in the future. While our research sheds light on the performance of the CC and ICC methods in time delay estimation, further experimental work is needed to fully evaluate their efficacy. Future research could also look into how these methods perform under different operating conditions or with different types of signals.

REFERENCES

[1] L. Duan, J. Hu, G. Zhao, K. Chen, J. He, and S. X. Wang, "Identification of partial discharge defects based on deep learning method," *IEEE Transactions on Power Delivery*, vol. 34, no. 4, pp. 1557–1568, Aug. 2019, doi: 10.1109/TPWRD.2019.2910583.

[2] E. Gulski *et al.*, "On-site testing and PD diagnosis of high voltage power cables," *IEEE Transactions on Dielectrics and Electrical Insulation*, vol. 15, no. 6, pp. 1691–1700, Dec. 2008, doi: 10.1109/TDEI.2008.4712673.

[3] M. N. K. H. Rohani *et al.*, "Classification of partial discharge detection technique in high voltage power component: A review," *International Journal of Integrated Engineering*, vol. 11, no. 4, Sep. 2019, doi: 10.30880/ijie.2019.11.04.027.

[4] E. P. Waldi, A. I. Lestari, R. Fernandez, S. Mulyadi, Y. Murakami, and N. Hozumi, "Rogowski coil sensor in the digitization process to detect partial discharge," *TELKOMNIKA (Telecommunication Computing Electronics and Control)*, vol. 18, no. 2, pp. 1062–1071, Apr. 2020, doi: 10.12928/telkomnika.v18i2.14282.

[5] M. I. Sharif, J. P. Li, and A. Sharif, "A noise reduction based wavelet denoising system for partial discharge signal," *Wireless Personal Communications*, vol. 108, no. 3, pp. 1329–1343, Oct. 2019, doi: 10.1007/s11277-019-06471-2.

[6] Y. Tian, B. Qi, R. Zhuo, M. Fu, and C. Li, "Locating partial discharge source occurring on transformer bushing by using the improved TDoA method," in *2016 International Conference on Condition Monitoring and Diagnosis (CMD)*, Sep. 2016, pp. 144–147, doi: 10.1109/CMD.2016.7757796.

[7] Y. Li, D. Chen, L. Li, J. Zhang, G. Li, and H. Liu, "Study of comparison between ultra-high frequency (UHF) method and ultrasonic method on PD detection for GIS," *IOP Conference Series: Earth and Environmental Science*, vol. 94, Nov. 2017, doi: 10.1088/1755-1315/94/1/012086.

[8] H. Chai, B. T. Phung, and S. Mitchell, "Application of UHF sensors in power system equipment for partial discharge detection: A review," *Sensors*, vol. 19, no. 5, Feb. 2019, doi: 10.3390/s19051029.

[9] H. D. Ilkhechi and M. H. Samimi, "Applications of the acoustic method in partial discharge measurement: A review," *IEEE Transactions on Dielectrics and Electrical Insulation*, vol. 28, no. 1, pp. 42–51, Feb. 2021, doi: 10.1109/TDEI.2020.008985.

[10] H. Karami, F. Q. Aviolat, M. Azadifar, M. Rubinstein, and F. Rachidi, "Partial discharge localization in power transformers using acoustic time reversal," *Electric Power Systems Research*, vol. 206, May 2022, doi: 10.1016/j.epsr.2022.107801.

[11] A. H. M. Hashim *et al.*, "Partial discharge localization in oil through acoustic emission technique utilizing fuzzy logic," *IEEE Transactions on Dielectrics and Electrical Insulation*, 2022, doi: 10.1109/TDEI.2022.3157911.

[12] Y. Zang *et al.*, "Optical detection method for partial discharge of printed circuit boards in electrified aircraft under various pressures and voltages," *IEEE Transactions on Transportation Electrification*, vol. 8, no. 4, pp. 4668–4677, Dec. 2022, doi: 10.1109/TTE.2022.3191308.

[13] O. Sefl, R. Prochazka, R. Haller, and G. J. Monkman, "Alternative approach to optical detection of partial discharges in air," in *2021 IEEE Conference on Electrical Insulation and Dielectric Phenomena (CEIDP)*, Dec. 2021, pp. 324–327, doi: 10.1109/CEIDP50766.2021.9705350.

[14] A. R. Mor, P. H. F. Morshuis, P. Llovera, V. Fuster, and A. Quijano, "Localization techniques of partial discharges at cable ends in off-line single-sided partial discharge cable measurements," *IEEE Transactions on Dielectrics and Electrical Insulation*, vol. 23, no. 1, pp. 428–434, Feb. 2016, doi: 10.1109/TDEI.2015.005395.

[15] H. Ha, S. Han, and J. Lee, "Fault detection on transmission lines using a microphone array and an infrared thermal

imaging camera," *IEEE Transactions on Instrumentation and Measurement*, vol. 61, no. 1, pp. 267–275, Jan. 2012, doi: 10.1109/TIM.2011.2159322.

[16] M. M. Yaacob, M. A. Alsaedi, J. R. Rashed, A. M. Dakhil, and S. F. Atyah, "Review on partial discharge detection techniques related to high voltage power equipment using different sensors," *Photonic Sensors*, vol. 4, no. 4, pp. 325–337, Dec. 2014, doi: 10.1007/s13320-014-0146-7.

[17] C. P. Beura, M. Beltle, and S. Tenbohlen, "Study of the influence of winding and sensor design on ultra-high frequency partial discharge signals in power transformers," *Sensors*, vol. 20, no. 18, Sep. 2020, doi: 10.3390/s20185113.

[18] H. Li *et al.*, "Fiber optic Fabry–Perot sensor that can amplify ultrasonic wave for an enhanced partial discharge detection," *Scientific Reports*, vol. 11, no. 1, Apr. 2021, doi: 10.1038/s41598-021-88144-4.

[19] B. A. de Castro, V. V. dos Santos, G. B. Lucas, J. A. Ardila-Rey, R. R. Riehl, and A. L. Andreoli, "A comparative analysis applied to the partial discharges identification in dry-type transformers by hall and acoustic emission sensors," *Sensors*, vol. 22, no. 5, Feb. 2022, doi: 10.3390/s22051716.

[20] A. Rodrigo-Mor, F. A. Muñoz, and L. C. Castro-Heredia, "Principles of charge estimation methods using high-frequency current transformer sensors in partial discharge measurements," *Sensors*, vol. 20, no. 9, Apr. 2020, doi: 10.3390/s20092520.

[21] M. Chojowski, M. Baszyński, R. Sosnowski, and A. Dziadecki, "High-frequency current transformers cascade for power electronics measurements," *Sensors*, vol. 22, no. 15, Aug. 2022, doi: 10.3390/s22155846.

[22] M. Fritsch and M. Wolter, "High-frequency current transformer design and construction guide," *IEEE Transactions on Instrumentation and Measurement*, vol. 71, pp. 1–9, 2022, doi: 10.1109/TIM.2022.3177189.

[23] Y. Shi, Z. Xin, P. C. Loh, and F. Blaabjerg, "A review of traditional helical to recent miniaturized printed circuit board Rogowski coils for power-electronic applications," *IEEE Transactions on Power Electronics*, vol. 35, no. 11, pp. 12207–12222, Nov. 2020, doi: 10.1109/TPEL.2020.2984055.

[24] M. V. R. Moreno, G. Robles, R. Albarracín, J. A. Rey, and J. M. M. Tarifa, "Study on the self-integration of a Rogowski coil used in the measurement of partial discharges pulses," *Electrical Engineering*, vol. 99, no. 3, pp. 817–826, Sep. 2017, doi: 10.1007/s00202-016-0456-4.

[25] H. Mohammadi and F. Haghjoo, "Distributed capacitive sensors for partial discharge detection and defective region identification in power transformers," *IEEE Sensors Journal*, vol. 17, no. 6, pp. 1626–1634, Mar. 2017, doi: 10.1109/JSEN.2017.2651028.

[26] S. Barrios, D. Buldain, M. P. Comech, I. Gilbert, and I. Orue, "Partial discharge classification using deep learning methods—survey of recent progress," *Energies*, vol. 12, no. 13, Jun. 2019, doi: 10.3390/en12132485.

[27] T. Sukumar, G. Balaji, B. Vigneshwaran, A. Prince, and S. P. Kumar, "Recognition of single and multiple partial discharge patterns using deep learning algorithm," in *2021 International Conference on Artificial Intelligence and Smart Systems (ICAIS)*, Mar. 2021, pp. 184–189, doi: 10.1109/ICAIS50930.2021.9395881.

[28] G. V. R. Xavier, A. C. de Oliveira, A. D. C. Silva, L. A. M. M. Nobrega, E. G. da Costa, and A. J. R. Serres, "Application of time difference of arrival methods in the localization of partial discharge sources detected using bio-inspired UHF sensors," *IEEE Sensors Journal*, vol. 21, no. 2, pp. 1947–1956, Jan. 2021, doi: 10.1109/JSEN.2020.3019760.

[29] Z. Li, L. Luo, N. Zhou, G. Sheng, and X. Jiang, "A novel partial discharge localization method in substation based on a wireless UHF sensor array," *Sensors*, vol. 17, no. 8, Aug. 2017, doi: 10.3390/s17081909.

[30] Z. Li, L. Luo, Y. Liu, G. Sheng, and X. Jiang, "UHF partial discharge localization algorithm based on compressed sensing," *IEEE Transactions on Dielectrics and Electrical Insulation*, vol. 25, no. 1, pp. 21–29, Feb. 2018, doi: 10.1109/TDEI.2018.006611.

[31] U. F. Khan *et al.*, "An efficient algorithm for partial discharge localization in high-voltage systems using received signal strength," *Sensors*, vol. 18, no. 11, Nov. 2018, doi: 10.3390/s18114000.

[32] S. Wang, Y. He, B. Yin, W. Zeng, Y. Deng, and Z. Hu, "A partial discharge localization method in transformers based on linear conversion and density peak clustering," *IEEE Access*, vol. 9, pp. 7447–7459, 2021, doi: 10.1109/ACCESS.2021.3049558.

[33] M. Isa, N. I. Elkalashy, M. Lehtonen, G. M. Hashmi, and M. S. Elmusrati, "Multi-end correlation-based PD location technique for medium voltage covered-conductor lines," *IEEE Transactions on Dielectrics and Electrical Insulation*, vol. 19, no. 3, pp. 936–946, Jun. 2012, doi: 10.1109/TDEI.2012.6215097.

[34] C. C. Yii, M. N. K. H. Rohani, M. Isa, and S. I. S. Hassan, "Multi-end PD location algorithm using segmented correlation and trimmed mean data filtering techniques for MV underground cable," *IEEE Transactions on Dielectrics and Electrical Insulation*, vol. 24, no. 1, pp. 92–98, Feb. 2017, doi: 10.1109/TDEI.2016.005902.

[35] G.-P. Kousiopoulos, G.-N. Papastavrou, D. Kampelopoulos, N. Karagiorgos, and S. Nikolaidis, "Comparison of time delay estimation methods used for fast pipeline leak localization in high-noise environment," *Technologies*, vol. 8, no. 2, May 2020, doi: 10.3390/technologies8020027.

[36] B. Anitha and C. Koley, "Time delay estimation of ultra high frequency signals radiated from partial discharge sources," in *2018 IEEE Applied Signal Processing Conference (ASPCON)*, Dec. 2018, pp. 188–192, doi: 10.1109/ASPCON.2018.8748867.

[37] M. N. K. H. Rohani *et al.*, "Effect of unshielded and shielded Rogowski coil sensor performance for partial discharge measurement," in *2015 IEEE Student Conference on Research and Development (SCOReD)*, Dec. 2015, pp. 21–25, doi: 10.1109/SCORED.2015.7449325.

[38] M. N. K. H. Rohani *et al.*, "Geometrical shapes impact on the performance of ABS-based coreless inductive sensors for PD measurement in HV power cables," *IEEE Sensors Journal*, vol. 16, no. 17, pp. 6625–6632, Sep. 2016, doi: 10.1109/JSEN.2016.2586302.

[39] A. A. Bakar, C. C. Yii, C. K. Fern, Y. H. Pin, H. Lago, and M. N. K. H. Rohani, "A comparison of double-end partial discharge localization algorithms in power cables," *Energies*, vol. 16, no. 4, Feb. 2023, doi: 10.3390/en16041817.
[40] A. A. Khan, N. Malik, A. Al-Arainy, and S. Alghuweinem, "Investigation of attenuation characteristics of PD pulse during propagation in XLPE cable," in *2013 IEEE Power & Energy Society General Meeting*, 2013, pp. 1–5, doi: 10.1109/PESMG.2013.6672724.
[41] A. Lyon, "Why are normal distributions normal?," *The British Journal for the Philosophy of Science*, vol. 65, no. 3, pp. 621–649, Sep. 2014, doi: 10.1093/bjps/axs046.
[42] S. Sun, S. Li, L. Lin, Y. Yuan, and M. Li, "A novel signal processing method based on cross-correlation and interpolation for ToF measurement," in *2019 IEEE 4th International Conference on Signal and Image Processing (ICSIP)*, Jul. 2019, pp. 664–668, doi: 10.1109/SIPROCESS.2019.8868700.
[43] C. Lingfeng, W. Yue, Z. Xiaodi, and L. Jiaming, "Research on the digital test of TV camera's signal to noise ratio," in *2007 8th International Conference on Electronic Measurement and Instruments*, Aug. 2007, pp. 3–869, doi: 10.1109/ICEMI.2007.4351055.

BIOGRAPHIES OF AUTHORS

Chin Kui Fern ⓘ � SC 🔵 is a dedicated academic and researcher in the field of Electrical Electronics Engineering. She holds a Bachelor of Engineering (Hons) in Electronics and Telecommunications Engineering from the University Malaysia Sarawak (UNIMAS) and an M.Eng. in Digital Electronics. With over a decade of experience in a PCB manufacturing company, she is a registered professional engineer. She is currently pursuing her Ph.D. in the Faculty of Engineering at the University Malaysia Sabah, where she is expanding her knowledge and skills in electrical engineering, with a particular focus on partial discharge detection, measurement, and location techniques. For any inquiries, please contact her at ckfern@icats.edu.my.

Chai Chang Yii ⓘ 🔵 SC 🔵 is a distinguished researcher and academic with expertise in Electrical System Engineering. He obtained his B.Eng. (Hons) in Electrical System Engineering from the University Malaysia Perlis (UniMAP) in 2013 and continued his academic journey to pursue his PhD from the same institution in 2017. His research interests include partial discharge measurement, detection, and location techniques, as well as power system transient studies. Chai has published extensively in these fields, and he is currently a senior lecturer at the University Malaysia Sabah. For inquiries or collaboration, kindly reach him through email at chaichangyii@ums.edu.my.

Asfarina Abu Bakar ⓘ 🔵 SC 🔵 is a highly motivated researcher with a keen interest in high voltage and renewable energy. She earned her B.Eng. in Electrical Engineering (Hons) from the University Tun Hussein Onn Malaysia (UTHM), Malaysia in 2012. Currently, Asfarina is pursuing her master's degree in the Faculty of Engineering at the University Malaysia Sabah. Her research interests are primarily focused on renewable energy, where she has already built a strong foundation in electrical engineering. To make any inquiries, kindly contact Asfarina through email at asfarina@icats.edu.my.

Ismail Saad ⓘ 🔵 SC 🔵 is an accomplished academic and researcher specializing in electronics and micro/nanoelectronics. He holds a BEng (Hons) in Electronics/Computer Engineering from the University Putra Malaysia, an MSc in Microelectronics System Design from the University of Southampton, and a Doctorate in Micro and Nanoelectronics Device and Material from the University Technology Malaysia, which provide him with a strong academic foundation. His research interests encompass nanofiber for energy applications, nano-biosensors, medical and healthcare systems, and nano-devices, and he has published extensively in these areas, demonstrating his passion for contributing to the electronics field. As an Associate Professor and Dean of the Faculty of Engineering, Ismail Saad has made significant contributions to electronics and nurtured a culture of academic excellence, innovation, and ongoing learning. To contact him for inquiries or collaboration opportunities, please email him at ismail_s@ums.edu.my.
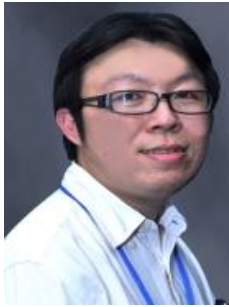
Kenneth Teo Tze Kin 🆔 🔗 SC ⟳ is a distinguished researcher in electrical and electronic engineering, holding a B.Eng. (Hons.) from the University of Leicester, and an M.Sc. and Ph.D. from Universiti Malaysia Sabah (UMS). As an Associate Professor and Deputy Dean of Engineering at UMS, he has established himself as a respected leader in his field, with research interests spanning over two decades in the areas of precision optimization and artificial intelligence. He has made significant contributions to smart energy, intelligent transportation, precision automation, analytical mechatronics, and biomedical science. His outstanding research excellence is reflected in his publications in high-impact journals. To contact him for inquiries or collaboration opportunities, please email kenteo@ums.edu.my.

Megat Muhammad Ikhsan Megat Hasnan 🆔 🔗 SC ⟳ is a senior lecturer at the Faculty of Engineering at Universiti Malaysia Sabah, and possesses a strong academic background. He received his Bachelor's degree in Telecommunication Engineering in 2011 and a Master's degree in Microelectromechanical Systems (MEMs) design from the University of Malaya. In 2019, he completed his Ph.D. Eng. Sci. in Renewable Energy, also from the University of Malaya. His research interests lie in the development of energy harvester materials and devices, smart sensors, and green energy. To reach him for inquiries or collaboration opportunities, he can be contacted at megatikhsan@ums.edu.my.

Nur Aqilah Mohamad 🆔 🔗 SC ⟳ is an accomplished senior lecturer at the University of Sabah in Malaysia. She received her B.Eng in Electrical & Electronics Engineering in Power from Universiti Pertahanan Nasional Malaysia in 2013. In 2016, she obtained her Master of Science in Electrical Power Engineering from Universiti Putra Malaysia and later completed her Ph.D. in 2021 from the same university. Nur Aqilah's research interests include transformer condition monitoring, insulation aging and diagnostics, and alternative high-voltage power equipment insulation materials. For any inquiries, kindly contact Nur Aqilah at nuraqilah.mohamad@ums.edu.my.